Available online at www.sciencedirect.com
SCIENCE DIRECT®
Deep-Sea Research I 52 (2005) 621–646
DEEP-SEA RESEARCH PART I
www.elsevier.com/locate/dsr

Winter upper ocean circulation in the Western Iberian Basin—Fronts, Eddies and Poleward Flows: an overview

Álvaro Peliz[a,*], Jesús Dubert[a], A. Miguel P. Santos[b], Paulo B. Oliveira[b], Bernard Le Cann[c]

[a]*Departamento de Física (Centro de Estudos do Ambiente e do Mar), Universidade de Aveiro, 3810-194 Aveiro, Portugal*
[b]*Instituto Nacional de Investigação Agrária e das Pescas-IPIMAR, Av.Brasilia s/n, 1449-006 Lisboa, Portugal*
[c]*Laboratoire de Physique des Océans, CNRS/IFREMER/UBO, UFR Sciences 6, Av. Le Gorgeu, C.S. 93837, 29238 Brest Cedex 3, France*

Received 10 November 2003; received in revised form 13 August 2004; accepted 1 November 2004

Abstract

An overview of the winter circulation and upper ocean structure offshore of Western Iberia is presented. The focus is on winter slope currents, fronts and mesoscale eddies, as well as on the connection of these local features to the large-scale circulation of the region. Satellite sea surface temperature; sea surface elevation data from altimetry; cross-shore and meridional hydrological surveys and current meter observations, mainly obtained during winter periods, are used to illustrate features of the winter upper ocean structure and of the generation and evolution of the Iberia Poleward Current. A schematic/hypothetical model of winter upper ocean circulation on the scale of the Western Iberian Basin is given which attempts to systematize and resolve certain ambiguities in the existing circulation schemes and in the concepts and terminology used to describe observed features in the area.

Keywords: Iberian Basin; Iberian Poleward Current; Western Iberia Winter Fronts; Portugal Current; Azores Current; Swoddies

1. Introduction

The Iberian Basin (Fig. 1) comprises the Iberian Abyssal Plain and the Tejo Abyssal Plain; it is limited to the north by the Galicia Bank (~ 1000 m), and to the south by the Tore Madeira Ridge and the Gorringe Sea Mount (at locations shallower than 200 m). The western limit of the basin is at approximately 16°W (taking the Tore Madeira Ridge as the western end) and the eastern limit is the meridionally aligned margin of Western Iberia. The main connection linking the basin and the Gulf of Cadiz is a passage (~ 4000 m) that runs between the Gorringe Sea Mount and the coast (at 37°N). A similar connection (shallower than

*Corresponding author. Tel.: +351 214412551.
E-mail address: apeliz@fis.ua.pt (A. Peliz).

0967-0637/$ - see front matter © 2005 Elsevier Ltd. All rights reserved.
doi:10.1016/j.dsr.2004.11.005

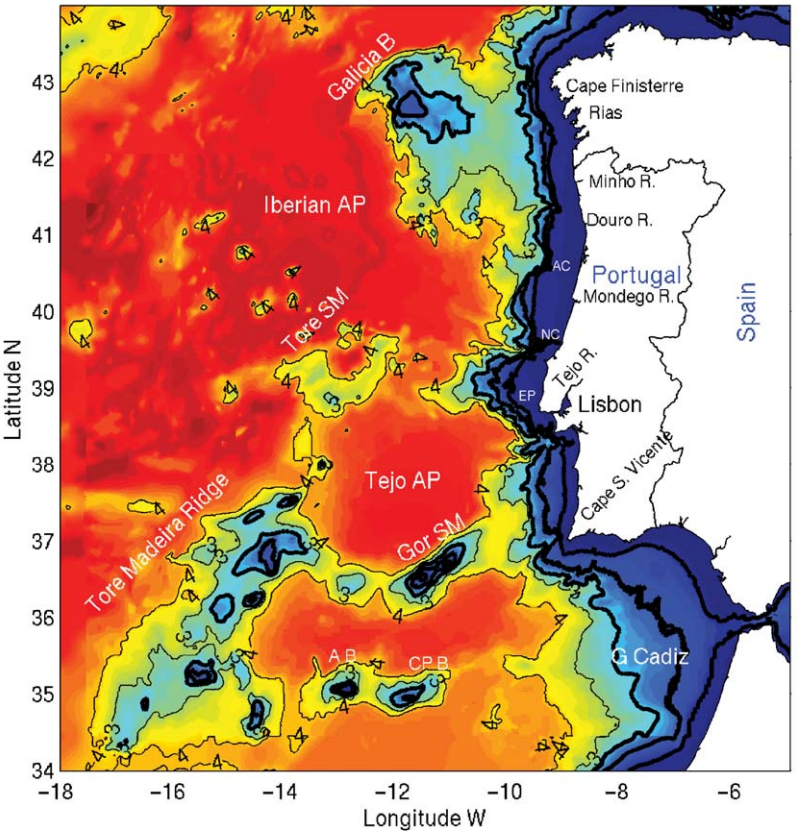

Fig. 1. Western Iberian Basin. Colors represent depth (red color for deeper zones). The isobaths correspond to 0.2, 1, 2 (thick lines), 3 and 4 km (thinner lines). Some of the main topographic features are indicated: the Iberian Abyssal Plain (AP), the Tejo Abyssal Plain, the Galicia Bank, the Tore Seamount (Tore SM), the Tore-Madeira Ridge (TMR), and the Gorringe Seamount (Gor SM). South of the Iberian Peninsula the Gulf of Cadiz (G. Cadiz) and to the west several banks including the Ampere Bank (AP) and the Coral Patch Bank (CPB). Other significant topographic structures in the western margin are indicated: The Estremadura Promontory (EP), and the Nazaré and Aveiro Canyons (NC and AC).

3000 m) with the Bay of Biscay exists at the northern end of the basin (43°N) between the Galicia Bank and the Galician coast.

The continental margin includes the western coasts of Portugal and Spain. South of the Estremadura Promontory (39°N) the shelf is narrow (~ 25 km) and the slope is not very steep. To the north of that latitude the shelf is wider (50–60 km) and several canyons cut the very steep slope. The narrow deep canyon of Nazaré and the wide canyon of Aveiro are the most notable. North of 41°N the shelf narrows again. River runoff is significant to the north of Lisbon where several rivers contribute fresh water input to the shelf. The Tagus, Douro and Minho are the most significant though other smaller rivers and lagoons, and also the Rías (in the northwest of Spain), contribute as well.

The Western Iberia Basin is known in the oceanographic literature for two major reasons: firstly, it constitutes the northern limit of the Eastern North Atlantic Upwelling Region, with strong and recurrent filament activity (Haynes et al., 1993); second, it contains the main pathway of circulation of Mediterranean Water into the Atlantic, which tends to follow the contours of the Portuguese southwestern slope, generating mesoscale features called Meddies (Armi and

Stommel, 1983; Richardson et al., 2000; Serra and Ambar, 2002).

At the beginning of the 1990s, the existence of poleward slope-flows during the winter period was described. The poleward flows were attributed to the seasonal reversal of the wind regimes, and to the response of the slope waters to meridional density gradients (e.g., Frouin et al., 1990). It was hypothesized that the poleward flow off western Iberia could also be connected to a northward recirculation of the Azores Current; this would explain the different characteristics (higher salinities) of Eastern North Atlantic Central Water (ENACW) in the northwestern part of the Iberian margin (Ríos et al., 1992). However, in some basin scale models the predicted circulation is predominantly southward at these latitudes (e.g., Paillet and Mercier, 1997; Mauritzen et al., 2001), and the poleward currents are restricted to the slope, where they are not significant in the transport budget. The generation of the poleward flow is associated with the interaction of the meridional density gradients with the coast, with the wind driven dynamics or with a recirculation of the Azores Current northeastward. However, the existing works are contradictory in some respects.

The origin, extent, and variability of the poleward flow itself is still not clear. It has been described as a narrow, upper slope trapped current weakening or even reversing by the action of southward winds. Modelling work by Peliz et al. (2003b) on the mechanisms of forcing of the IPC demonstrate that density forcing may oppose the wind-driven currents.

The purpose of this study is to summarize the main achievements regarding the understanding of the structure of the winter circulation of the Western Iberian Basin; and also to present new results based on unpublished data, focusing on the generation and characteristics of the IPC, its variability and relation to the large scale circulation of the area. The upper ocean structure and poleward flows along the Western Iberian slope are discussed, and a circulation scheme is proposed as an attempt to systematize terminology and concepts, as well as to resolve ambiguities regarding circulation features identified and described in other papers.

2. Large scale and boundary circulation in the Western Iberian Basin

The large-scale circulation in the North-Eastern Atlantic (NEA) is dominated by two basin-scale currents: The North Atlantic Current (NAC) extension to the north of the Iberian Peninsula (48–53°N) and the Azores Current (AC) south of Iberia centered at about 34–35°N. This inter-gyre region has been defined as having a weak circulation (e.g., Pollard and Pu, 1985), and according to certain circulation schemes (e.g., Krauss, 1986; Sy, 1988; Brügge, 1995) based on buoy data and analysis of hydrography fields, the two gyres are connected by a slow southward advection which Saunders (1982) named the Portugal Current.

According to Ríos et al. (1992), off northwestern Iberia the upper layers (0–300 m) of ENACW are saltier than expected for those latitudes. The authors hypothesized that these waters originate north of the Subtropical Front/Azores Current system (STF/AC) and are advected northward. This finding is in apparent contradiction with the extension of the Portugal Current to the longitudes of the Western Iberia Basin.

Recent papers (Paillet and Mercier, 1997; Van Aken, 2001; Penduff et al., 2001) agree that the basin-scale inter-gyre circulation is predominantly southward. As it moves south, Subpolar Mode Water (SPMW) subducts and secondary pycnoclines are generated (Paillet and Arhan, 1996). This process explains the difference in water mass characteristics in the upper layers of ENACW observed by Ríos et al. (1992). Penduff et al. (2001) suggest that during the winter period a poleward slope-flow off western Iberia may exist, but has no explicit expression in their model results. The absence of this feature from large-circulation models is either a result of its relatively short spatial scale or its seasonality.

Poleward flows along the Western Iberia margin were first described in detail by Frouin et al. (1990) and Haynes and Barton (1990). Later, a series of papers by Pingree and Le Cann (1992a, b, 1993) describe the poleward slope currents around northern Iberia and in the southern Bay of Biscay as an interconnected circulation process.

The only transport budget calculation based on observations on the scale of the Iberian Basin is presented by Mazé et al. (1997). They confirm the existence of a northward flow off western Iberia, at both Mediterranean and Central Water levels. Secondly, they demonstrate there is strong coupling of the transports of these two water masses in the sense that they usually have the same orientation. The transport through the northern boundary at 43°N between ~ 13°W and the coast amounts to 4.7 Sv. Part of this flow originates from the south, possibly as a recirculation of the AC from the Gulf of Cadiz. At 37°N (the southern boundary between the coast and ~ 12.5°W) it amounts to 1.9 Sv. 2.0 Sv enters from the west at about 12.5°W (between 37°N and 43°N). The remaining 0.7 Sv missing from the horizontal budget is attributed to diapycnal transport that contributes to the modification of Central Water properties by inducing an upward flux from Mediterranean Water levels.

Further contribution to the understanding of the circulation along the Iberian Margin was given by Van Aken (2001) and Pérez et al. (2001). Van Aken (2001) describes a large-scale southward advection offshore, though he does not exclude the possibility of a narrow poleward flow of warmer and saltier waters along the Iberian Peninsula coasts. Through a chemical study, Pérez et al. (2001) show that both advective processes coexist at the northern end of the Western Iberia margin: the southward transport of fresh ventilated waters by the Portugal Current and a northward advection of saltier and warmer water along the slope. Van Aken (2001) hypothesizes that the Central Water described by Ríos et al. (1992) is produced by poleward transport along the Iberian Peninsula, together with enhanced turbulence acting to increase diapycnal mixing.

A complementary contribution to the subject of higher salinities in ENACW is given by Mauritzen et al. (2001). These authors claim that the Mediterranean overflow downstream of the Strait of Gibraltar produces higher salinities in the Gulf of Cadiz surface waters through a detrainment process arising from the diapycnal mixing caused by vertical shear instabilities of the denser water flow (an upward salinity flux). The surface waters would then circulate westward and northward, promoting the salinity increase seen in Central Water off West Iberia.

The Azores Current and the Subtropical Front are usually observed south of 36°N (Paillet and Mercier, 1997; Pingree, 1997; Penduff et al., 2001). It is also commonly accepted that the AC mainly recirculates southward. For example, Pingree (1997) proposes a recirculation in two main branches: one west of Madeira and the other closer to the African coast. However, in this same study, the author presents observational evidence of a possible northward recirculation (see Pingree, 1997; buoy data corresponding to 1993). Models by both Paillet and Mercier (1997) and Penduff et al. (2001) only show southward recirculation paths, though a significant component of flow is still directed onshore into the Gulf of Cadiz. However, in these models the flow does not recirculate horizontally; instead it converges vertically into the deeper layers: as much as 4 Sv in the case of Paillet and Mercier (1997) and 1.5 Sv in the case of Penduff et al. (2001). The extension of the AC into the Gulf of Cadiz is also suggested in other papers (Jia, 2000; Mauritzen et al., 2001). In addition, Jia (2000) claims that the origin of the AC may be associated with the dynamics of the Mediterranean overflow. A modeling study supporting this link is described by Özgökmen et al. (2001).

New et al. (2001) present results of three different numerical modelling approaches for the North Atlantic. The three models each simulate Azores Currents with approximately the same origins and crossing the Atlantic at similar latitudes, though with different intensities and transports. However, the circulation at the eastern end of the AC and off the Iberian Coasts is significantly disparate (see their Fig. 1). In their isopycnal model, where the eastern branch of the AC seems to be better represented, there is a strong cyclonic recirculation of the flow: the current flows eastward until it meets the northern Moroccan coast, then skirts the continental margin northward along the southwest Iberian coast before turning back oceanwards at about 40°N. To our knowledge, no observational confirmation of this recirculation exists.

3. Data and methods

The CTD data that is presented in this work is all original and were collected within several IPIMAR (Portuguese sea and fisheries research agency) observational programs from 1996 to 1998. Several Seabird CTDs (19 and 9+) were used and the data were processed by standard procedures (Seasoft, Seabird technical reports-www.seabird.com) at IPIMAR.

Currentmeter data were provided by the Instituto Español de Oceanografia (Alonso et al., 1995). Hourly RCM 4 data were filtered to eliminate inertial and tidal frequencies with a 28-h half-amplitude period filter as described by Rosenfeld (1983), and then interpolated to 12-h intervals.

Frontal climatology was calculated with data from the NOAA/NASA Ocean Pathfinder Program (Smith et al., 1996), available at 9 km resolution from the Physical Oceanography Digital Active Archive Data Center at the Jet Propulsion Laboratory (Halpern, 1991). The data were used to construct maps of SST fronts with a single image edge detection algorithm (Cayula and Cornillon, 1992). This algorithm is derived from a combination of existing algorithms operating at local level and the regional level. At the regional level, the temperature distribution of overlapping 24×24 pixel windows is analysed to determine the statistical relevance of each possible front, while local operators are used to complete the contours found. Only the fronts representing a local temperature gradient greater than $0.5\,^{\circ}C/10\,km$ were retained in this study. To account for the large spatial and temporal variability in cloud cover, frontal probability images were computed. A frontal probability image shows the number of times each individual pixel is classified as a front divided by the number of times the pixel is clean, in other words the occurrences of fronts normalized by the number of observations. The frontal probability was computed for the winters (January–March) from 1985 to 2002.

The global SLA (Surface Level Anomaly) maps and mapping error distribution (Fig. 16) were produced by the CLS Space Oceanography division from a combination of Topex/Poseidon and ERS altimetry (Ducet et al., 2000). One map every 7 days from 1992 to 2002 is available on a Mercator $1/3^{\circ}$ grid. To increase the validity of the estimates we considered only those data with elevations larger than 2 cm and a mapping error value less than 35% (more restrictive criteria would eliminate a significant amount of data). The SLA maps are used to compute yearly composites of the number of winter (January–March) positive SLA occurrences. The obtained statistics do not correspond to a census of eddies since part of the elevations may correspond to wave-like patterns or meanders, and in some cases the same structure may have been surveyed several times such as in the case of westward propagating features. Note also that part of the surface elevation variability may be associated with eddy activity in the intermediate layers, such as meddies (Stammer et al., 1991; Oliveira et al., 2000). Nevertheless these distributions do give us useful information concerning eddy activity along the frontal systems.

4. Structure of the upper ocean off western Iberia

It has been shown in previous studies (e.g., Frouin et al., 1990; Peliz et al., 2003a, b) that a meridional density gradient is among the most important mechanisms in the generation of Eastern Poleward Currents, such as that observed along the Western Iberian Margin. Yet little is known about these density gradients and their variability.

Large scale surveys conducted in the Eastern North Atlantic do show a significant gradient in the density structure of the upper ocean at the latitudes of Western Iberia (Pollard and Pu, 1985; Arhan et al., 1994; Van Aken, 2001). Van Aken (2001) presents a climatological zonal average of the meridional density distribution in the upper ocean at 20°W. It is possible to observe in his Fig. 7 that the north–south density differences, at least at the latitudes of the Iberian Peninsula, are mainly limited to the upper 500 m. The scale of the meridional density gradient may vary as well. Pollard and Pu (1985) noted a small-scale ($\sim 100-200\,km$) meridional transition at about

40°N (see their Figs. 5 and 6). Similar frontal systems were also detected by Arhan et al. (1994) and Vitorino (1995).

4.1. Hydrological structure from CTD data

An example of the vertical distribution along a meridional north–south section taken at 12° (Sec W of Fig. 2 from IPIMAR cruise 02070598 of May 1998) is presented in Fig. 3. Note that the temperature is more than 2 °C lower in the northern end of the section. Although the salinity is also lower it does not compensate for the temperature difference and the water is denser to the north. A regular slope in the isopycnals is noticeable in the first 500 m. The core of the front is approximately located between 39 and 40°N which is coincident with the latitudes reported by Pollard and Pu (1985) and Vitorino (1995). At greater depths (below 600 m) the temperature and salinity distributions reveal the presence of meddies in the southern part of the section. The magnitude of the north–south density differences is 0.1–0.2 kg m^{-3} as in other meridional sections presented in the literature. Fig. 3d shows an estimate of the zonal geostrophic velocity with a reference depth at 800 m. Between 39 and 40°N, where the main meridional gradient is located, there is a 300–400 m deep coastward geostrophic flow with a core at about 39°N with velocities of

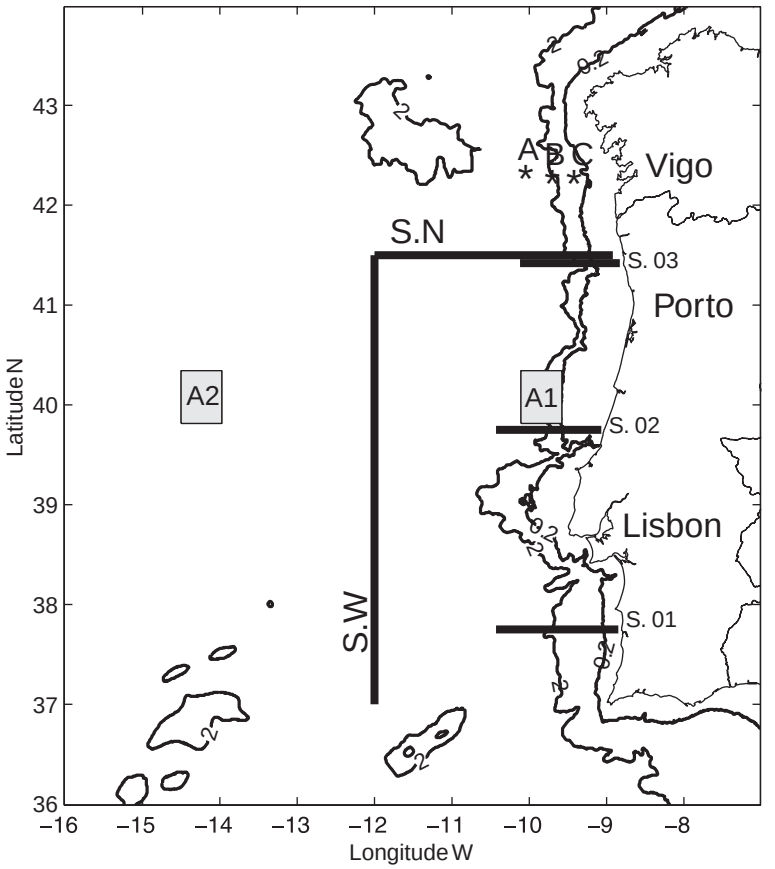

Fig. 2. Map with the location of data shown in other figures. Sections of IPIMAR cruise 02070598 (Sections N and W) of May 1998. Sections 01-03 repeated several times on different IPIMAR cruises. The moorings of the Spanish Oceanographic Institute (IEO) are represented with the letters A, B, and C offshore of Vigo (northwest Spain). SST time series from NOAA Pathfinder database were extracted and averaged for the locations A1, A2 indicated in the figure. The thick isobaths correspond to the 0.2 and 2 km depths.

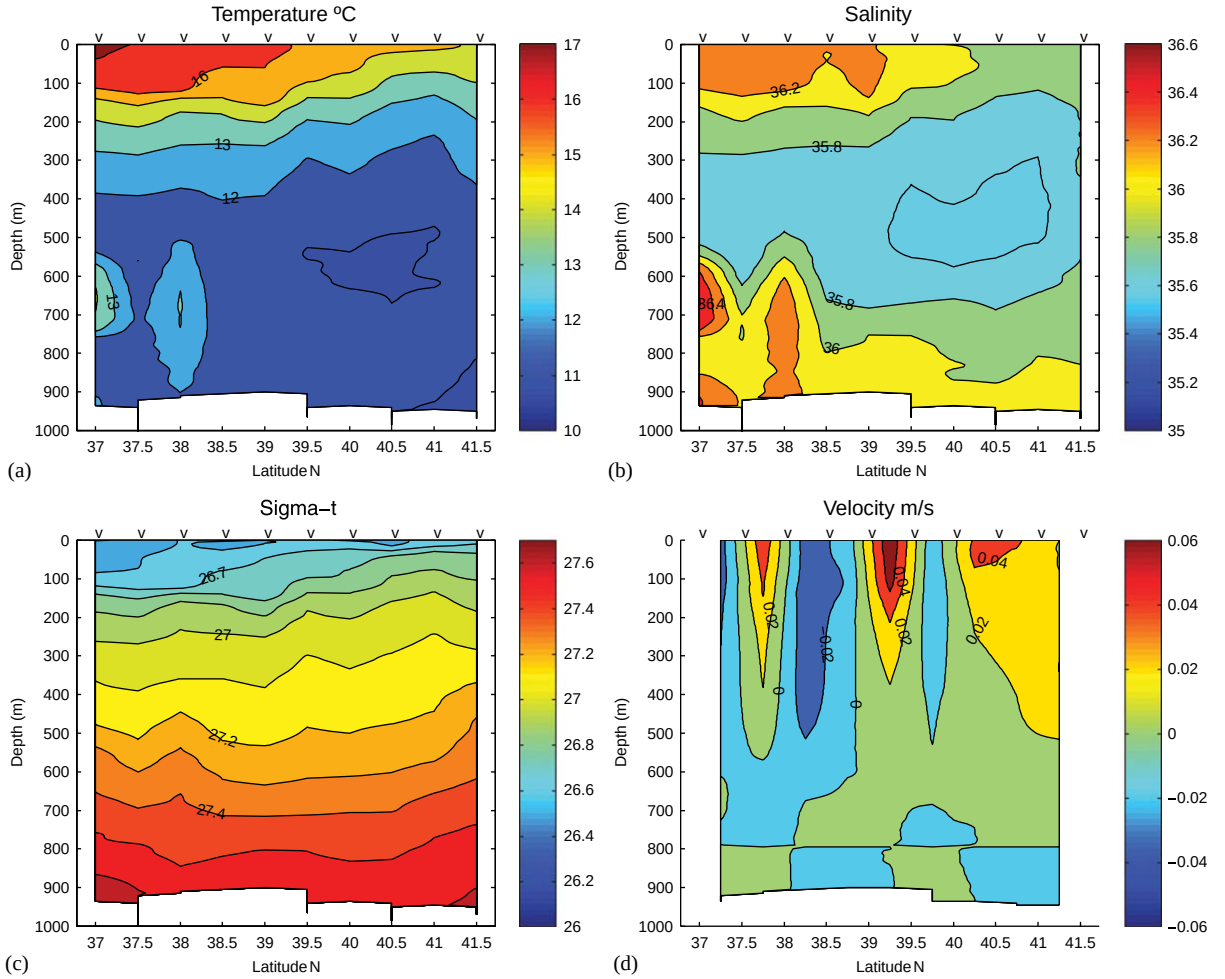

Fig. 3. North–south section along 12°W between 42°N and 37°N (S. W of Fig. 2) with the vertical distribution of: (a) temperature, (b) salinity, (c) density anomaly (kg m^{-3}), and (d) zonal geostrophic current with 800 m depth as reference level (m/s—positive values correspond to eastward flow). Data were collected during IPIMAR cruise 02070598, in May 1998.

around 6 cm/s. Values of this magnitude were obtained in the modeling study of Peliz et al. (2003a) using conditions for the density structure approximated to those of Fig. 3. Their results show that such a meridional gradient produces a coastward transport of above 1 Sv.

Fig. 4 shows the time-evolution of the density difference between the northern and southern locations offshore of Portugal on a quasi-monthly basis for 1996–1997. The data correspond to sections 01 and 03 of the IPIMAR-FITOX observational program (see Fig. 2). An average of the two westernmost density profiles from each section was first calculated, and then the difference between the averaged profiles was found. Unfortunately, the westernmost stations of the sections are not sufficiently distant from the coast to escape the influence of upwelling filament activity in summer. The significant variability in the gradient in the first tens of meters is possibly caused by local air–sea interaction or the presence of colder upwelled waters. To enhance the seasonality of the background gradient (in the Central Water) we show the data between 50 and 500 m.

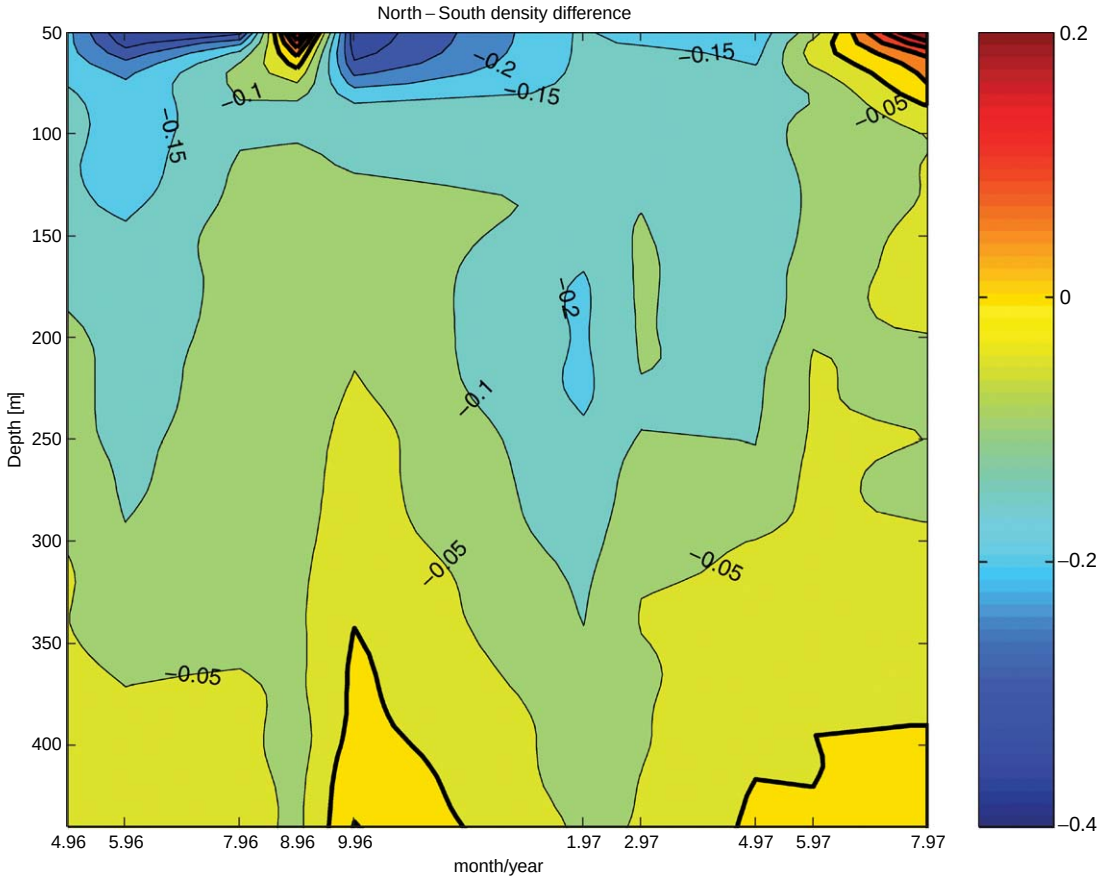

Fig. 4. Evolution (April 1996 to July 1997) of the upper 50–450 m density difference between the southern and northern part of Portugal. The plot was obtained by first averaging the two westernmost density profiles (stations) of each of the sections 01 and 03. Secondly the difference between the north and south mean profiles was calculated. Contours represent 0.05 kg m^{-3} intervals. The thicker lines correspond to positive values (southern waters heavier than northern ones).

The figure demonstrates that, with the exception of the surface layer during the peak of summer, a seasonal cycle is present in the meridional gradient expressed by an overall weakening of the north–south density difference during summer. However, the background difference is always around 0.05 kg m^{-3}, reaching values of 0.1–0.2 kg m^{-3} in the winter months, such as in January 1997.

4.2. Winter SST distribution and variability

Recurrent thermal gradients are observed in the winter infrared imagery of Western Iberia. Fig. 5 provides an exceptionally clean SST image to illustrate a synoptic surface thermal distribution. The image corresponds to a winter (February 1998) with particularly intense poleward flow.

The most noticeable feature is the front evolving along 40°N separating colder waters to the north from southern warmer waters. Gradient zones are perturbed by meandering structures of differing scales, and close to the coast these gradients are deflected northward generating a band of warm and turbulent features in the vicinity of the slope, approximately aligned along 10°W. Another particularly clear structure seems to be a developed instability or a northward intrusion along the 13°W meridian. West of 14°W the thermal

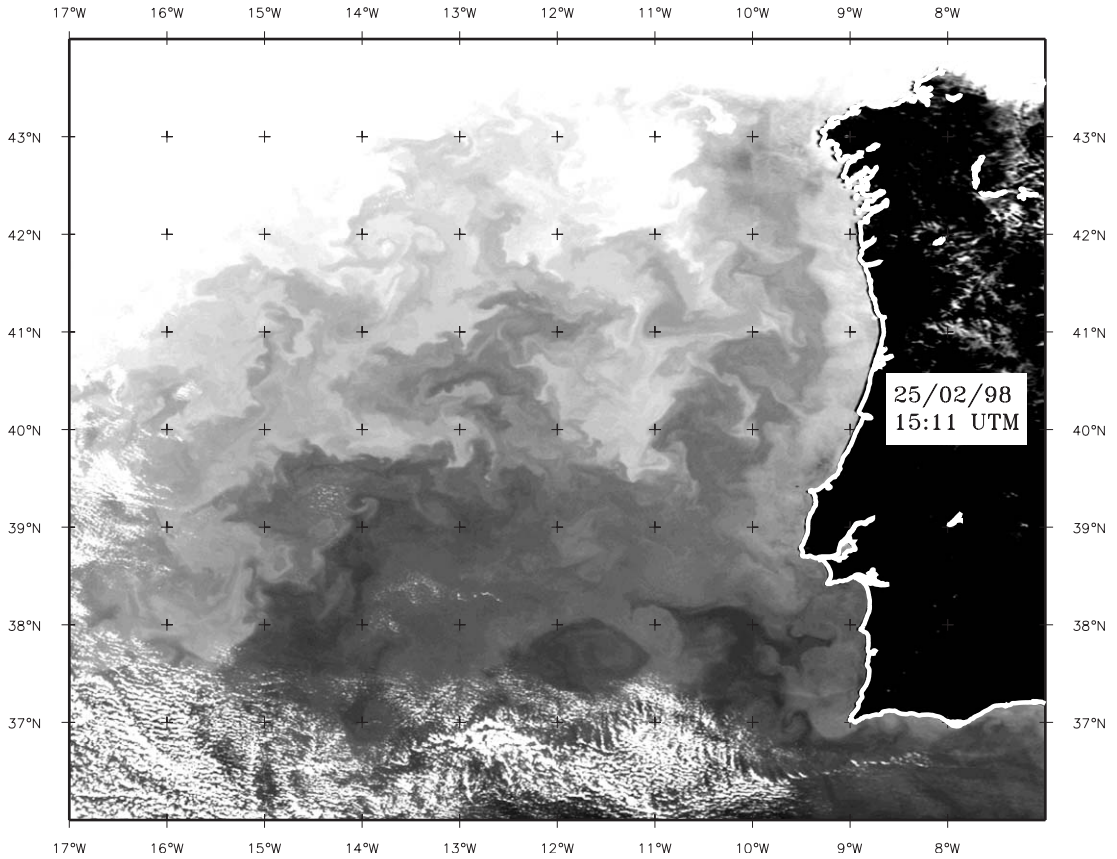

Fig. 5. Surface brightness temperature image (AVHRR 25/02/98 15:11 UTM) of the Western Iberian Basin. The darker tones correspond to warmer waters. The southwest portion of the image is partially affected by clouds (white patches). Linear stretching is used to enhance the circulation features.

gradient is deflected southwestward, the front appears to contour the Tore Madeira Ridge, turning coastward north of the Tore SM (see Fig. 1). To the south, several warmer (darker) features can be observed (37°N, 12°W); these are possibly linked to meandering extensions of the STF/AC. Thermal gradients such as these are recurrent in other SST images although they vary in meridional location and intensity.

To investigate the presence of SST fronts off western Iberia a probability of frontal occurrence was calculated (see Section 3). Fig. 6 presents the frontal probability for the whole period (1985–2002). It is evident that the zones of high probability of occurrence of SST fronts are organized in several quasi-zonal bands. One of these bands is located off Cape S. Vicent and is oriented soutwestward; a second contours the northern edge of the Estremadura Promontory; and two more can be seen between 40°N and the northwest tip of Iberia. The whole area east of 14°W appears to have a relatively high occurrence of fronts. The frontal probability off Western Iberia is even higher than the western zone south of 36°N where the influence of the Azores Current is expected to be most significant. The high frontal probability close to Cape S. Vicente is due to persistent local fronts between the shelf and deep waters, as is possible to conclude by examination of individual scenes.

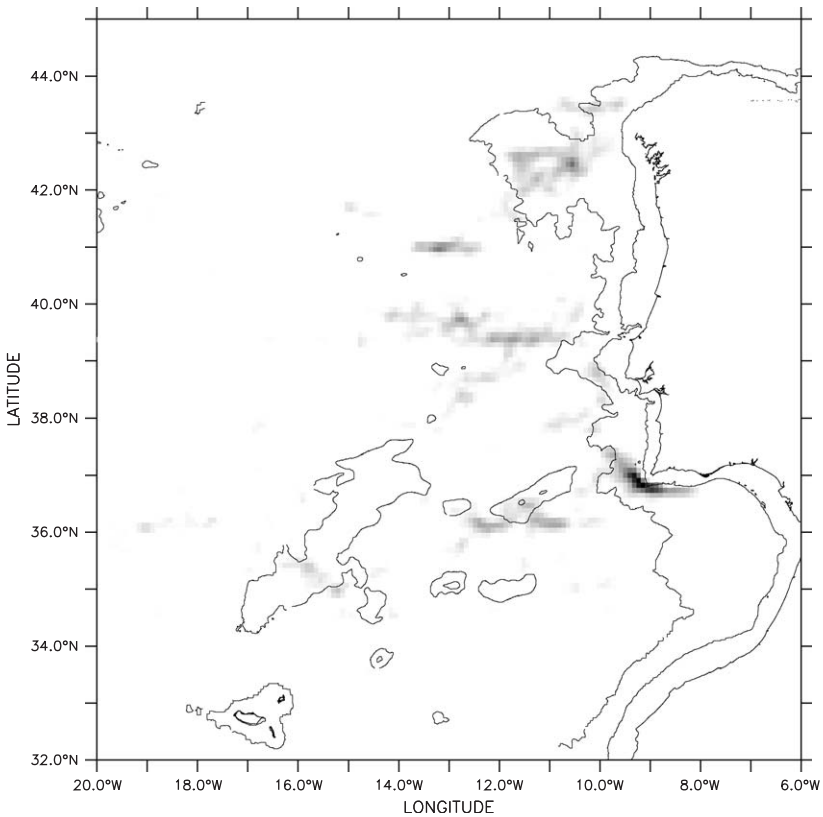

Fig. 6. Global frontal probability distribution for all winters (January–March) for the period 1985–2006. The 0.2 and 3 km isobaths are shown.

4.3. Interannual variability

Observations of individual satellite images indicate that in the years 1996–1998 and 2001, particularly intense poleward flows were experienced along Western Iberia. The presence of a warm tongue along the slope and eddy structures is recurrent in many of the SST distributions (Garcia-Soto et al., 2002, also report strong poleward flows for the years 1996 and 1998) whereas the years 1999 and 2000 do not show significant signatures of a poleward current.

Fig. 7 shows the evolution of winter values (averaged January and February) of zonal temperature gradient, meridional wind stress and North Atlantic Oscillation index (NAO) off western Iberia from 1985–2001. The thick line corresponds to the SST difference (NOAA/NASA - Pathfinder, monthly averages at 9 km) between the averages of areas A1 and A2 represented in Fig. 2. This zonal temperature difference is expected to be related to the intensity of poleward advection of southern warmer waters along the western Iberian coast. Positive values indicate that coastal temperatures are higher than those offshore, as for the years 1989–1990 and 1996–1998 and 2001.

Meridional wind stress winter averages (January and February) from NCEP data at 40°N, 12°W are represented by the dotted line. Positive values indicate convergence conditions (coastal poleward flow) and negative indicate upwelling-favourable events (coastal southward currents). The thick dash-dotted line represents the normalised NAO values (Jones et al., 1997) averaged for January and February. For the whole observed period no significant correlation between series was calculated (even NAO and wind stress are not

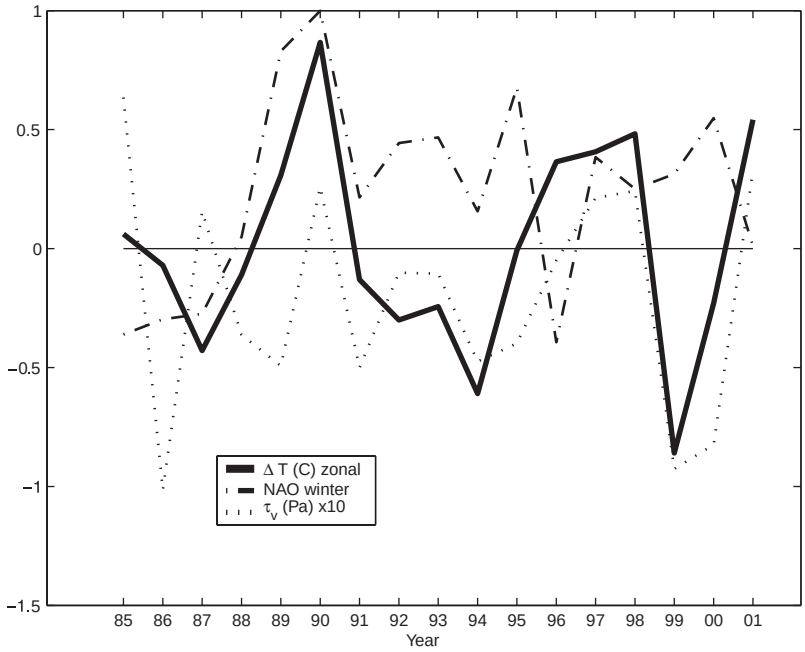

Fig. 7. Time series (1985–2001) of winter means (January–February) of different parameters. The thick solid line represents the evolution of the zonal SST difference (calculated between areas A1 and A2 of Fig. 2). The dotted line represents the winter averaged meridional wind stress (Pa × 10) from NCEP reanalysis. North Atlantic Oscillation index normalized values are represented by the dash-dotted line.

covarying). However, the zonal gradient and wind stress after 1994 show a high correlation (0.94; significant at 99% level). In the period before (1985–1994) the correlation is low (0.24). The inverse situation occurs for the SST gradient–NAO covariance. These series are marginally correlated (0.56; significant at 95% level) in the period 1985–1995 with no correlation after that period. Despite the high significance of the SST-wind stress correlation after 1994, this is a short period. Also, in situations of strong offshore Ekman transport the coastal buoyant waters cool at the surface and mask the signature of the IPC. This situation was reported for February 2000 by Santos et al. (2004). Garcia-Soto et al. (2002) suggest that years of strong warming off the northern coast of the Iberian Peninsula were associated with low NAO events. Our values do not confirm such a relationship between these variables for the western part of Iberia.

5. The Iberian Poleward Current

5.1. Current meter data

There is unfortunately a poor record of directly measured currents over the northwestern Iberia upper slope zone. Here, we make use of three existing datasets from the Instituto Español de Oceanografia (Alonso et al., 1995) to illustrate certain characteristics of the IPC.

Moorings were deployed in the northern part of the western Iberia slope off Vigo (see Fig. 2 at $\sim 42.5^{\circ}$N). The depths of the moorings were (A) 2700 m, (B) 2337 m and (C) 1338 m. Moorings B and C were above the slope (note that the slope is very steep in this zone) whereas A is about 30 km away from the 2000 m isobath (about 70 km off the shelf-break). Fig. 8 shows the record of the two current meters deployed on mooring A at 56 m (Fig. 8b) and 256 m (Fig. 8c) obtained between May 1993 and April 1994, and the corresponding

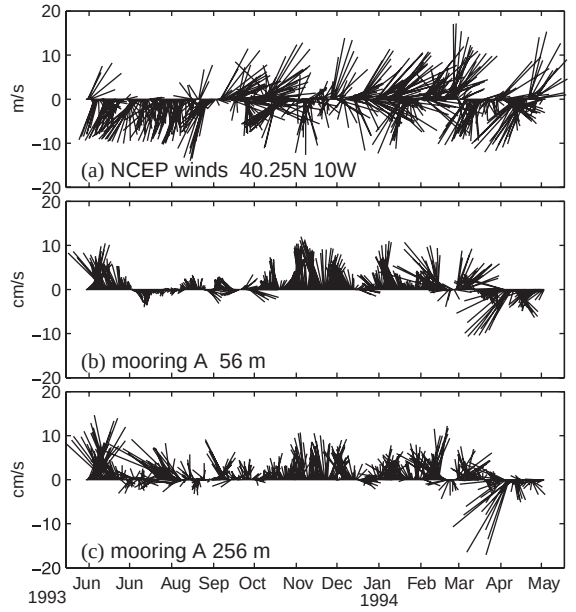

Fig. 8. Current meter records from June 1993 to May 1994 of mooring A (42.267°N, 10.15°W, at 2700 m depth; see Fig. 2): (b) at 56 m, and (c) at 256 m. (a) Corresponding winds from NCEP at 42.25°N, 10°W.

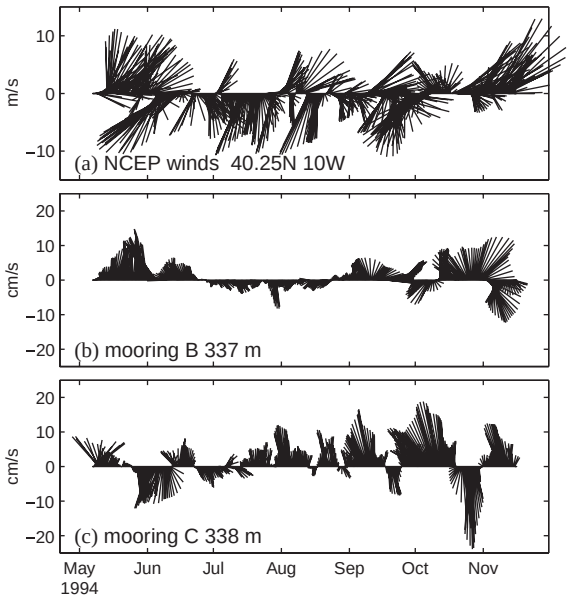

Fig. 9. Current meter records from May to November 1994 for: (b) mooring B (42.218°N, 9.802°W at 337 m at an ocean depth of 2337 m), and (c) mooring C (42.218°N, 9.509°W at 338 m at an ocean depth of 1338 m; see Fig. 2). (a) Corresponding winds from NCEP at 42.25°N, 10°W.

daily averaged winds (interpolated to 12-h intervals) from NCEP at 40.25°N, 10°W. Fig. 8b and c show low-passed currents subsampled every 12 h.

Since mooring A is somewhat distant from the slope it is not expected that the core of the poleward slope current was always being measured. However, the current is observed to be predominantly northward with intensities around 10 cm/s. Both current meters (56 and 256 m) show a weakening and at times reversing poleward flow in the period between July and October 1993. However, in the currents at 256 m the difference from the winter period is not so clear. The winds during the deployment period were predominantly northerly until late September, turning to west-southwesterly at the beginning of October. Correlation analysis did not reveal any significant covariance between winds and currents. However, it is clear that the change in the winds at the end of summer is coincident with more consistent poleward flow after that period.

Data from mooring A shows that despite the observations being taken 70 km off the shelf break, the IPC is still significant at these depths. The two observed layers have consistent poleward flow during most of the period (near 10 cm/s). The two layers decouple only in summer (July, August - likely in association with filament activity), but the northward component still dominates the currents at 256 m.

Moorings B and C had current meters at equal depths (about 340 m) for the period May–November 1994. Current vectors from these moorings are shown in Fig. 9, together with the NCEP winds for the same period taken from 40.25°N, 10°W.

During both May and November flow is more poleward in B showing that the strongest currents are not always trapped on the slope: the current at mooring C is weaker or variable during these periods. From June to late September the wind is southward (upwelling favourable). During July and August the current at B is southward. However, the current meter at mooring C (closer to the slope; note the significant polarization due to the topography) shows consistent northward orientation during this period.

Unfortunately the current meters were too deep to infer the surface flow. It is unlikely that the currents above the measured level in B were poleward. It is also not probable that the current is bounded near the shelf edge (the summer values in C are most probably associated with an upwelling counter-current). In this context, two scenarios for the fate of the IPC during summer 1994 may be considered: (i) the flow has reversed during July–August, or (ii) the IPC weakened and was advected offshore. The latter should not be eliminated given the results of mooring A (Fig. 8) where poleward flow was measured in the summer of the year before.

After September the rotation of the currents in both current meters may possibly be related to the presence of mesoscale features. No relation between the currents and local winds at zero lag or between moorings B and C at zero lag is apparent. However, lagged correlation analysis between current records and winds shows peaks of 0.35 (significant at the 95% confidence level) for phase lags of about 7 days with the winds leading the currents.

5.2. Winter 1997 IPC from in situ and satellite imagery

The across-slope temperature and salinity measurements taken during the FITOX program (see Fig. 2) in January 1997 are used to illustrate some of the characteristics of the poleward flow. Fig. 10 shows a surface temperature distribution (obtained from AVHRR data) that corresponds to the period of the in situ survey. The thick lines crossing the slope represent the location of the sections shown in Fig. 11.

In the satellite image, the current is visible as a warm intrusion that is broader in the south and proceeds northward with a meandering path (discussed below). In the northern zone, the lighter tones correspond to cold shelf waters of riverine origin which partially mask the signature of the slope flow. The two sections (Fig. 11) show the internal structure of the current. Note that the deflection of the isopycnal field is significant well beyond the slope zone and decreases substantially at 500 m. Between sections, the flow narrows from

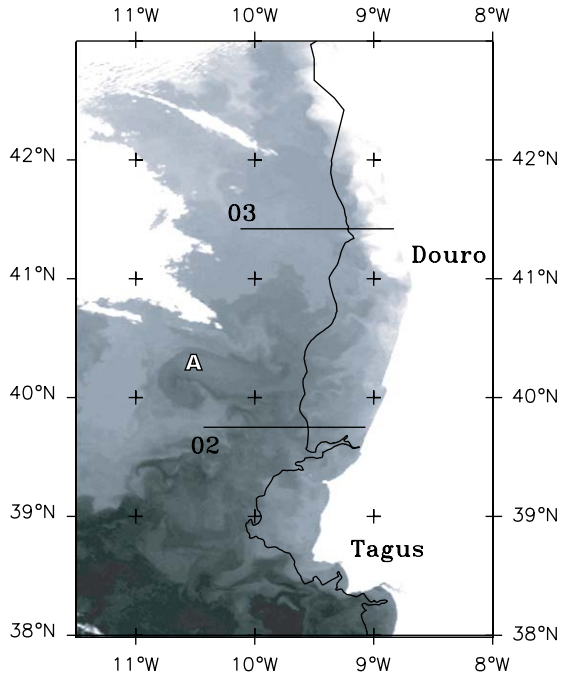

Fig. 10. AVHRR brightness temperature image of 28/01/97 (03:21 UTM) showing Western Iberian offshore. Darker tones correspond to warmer waters. The thicker zonal lines indicate the position of the sections shown in Fig. 11. Along the coast a white band corresponds to the colder WIBP waters. The center of an anticyclone is marked (A).

about 40–60 km in the south to 20–40 km in the north. At the northern section there is a warm and salty core on the upper slope which is isolated from the surface. This latter feature is sometimes observed in other sections and is associated with offshore spreading (driven by wind) and vertical mixing of the cold/fresh shelf waters with the warm/salty slope waters. This process may contribute to the isolation of a core of warm and salty water from the surface, as seen in the vicinity of the shelf break in the northern section.

Near shore (Fig. 11) a second stratified zone relates to buoyancy-driven circulation (of riverine origin) and is not influenced by the slope-flow. In fact, between the two zones a southward flow may even exist. Peliz et al. (2003a) found that a southward flow at the shelf break was associated with the baroclinic structure of the northward progressing warm tongue. This feature is linked to

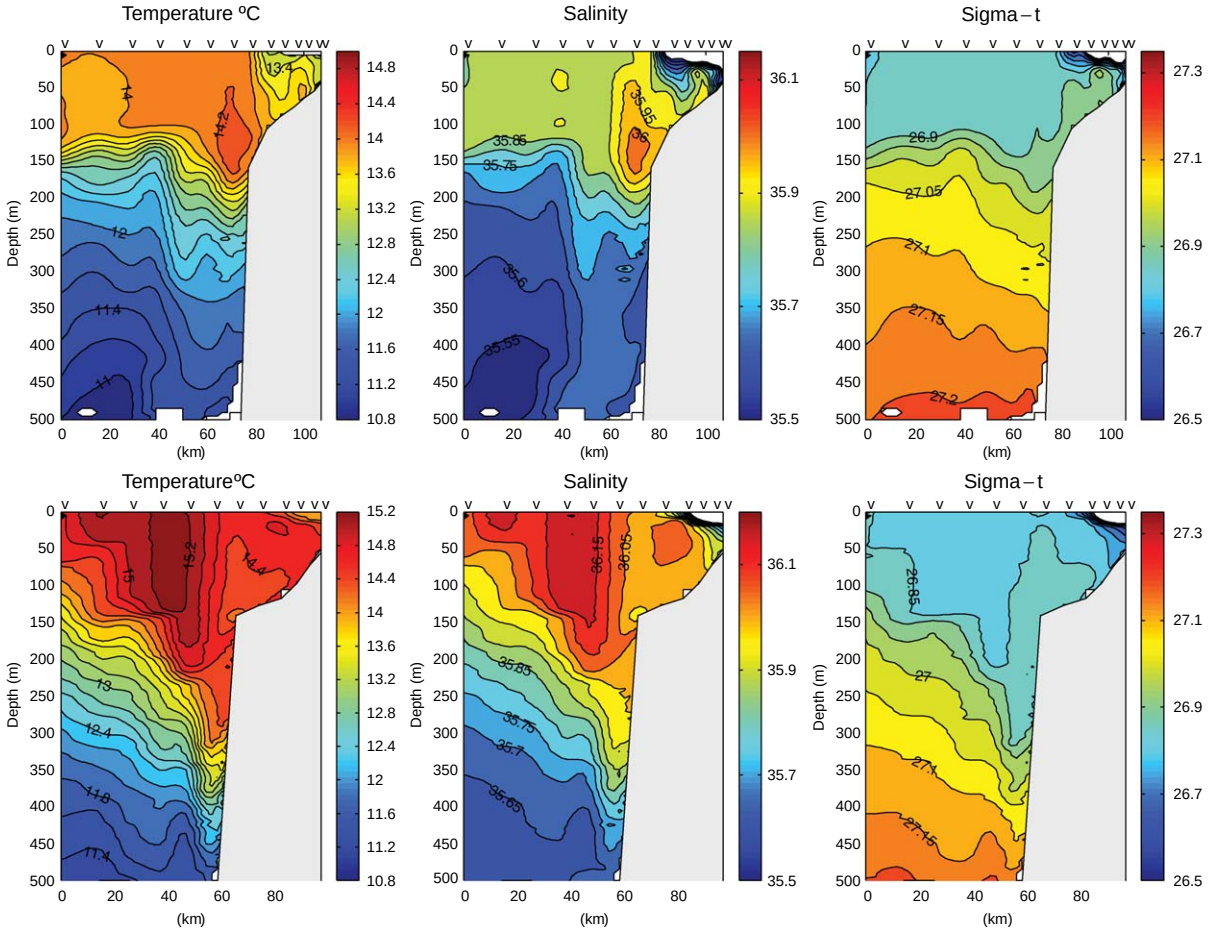

Fig. 11. Across-slope temperature, salinity and density anomaly (kg m^{-3}) vertical distributions for section 03 (upper row), and section 02 (lower row) measured on 26 and 27 February 1997. The dates of these sections are coincident with the SST image shown in Fig. 10 and their location is therein indicated.

the rise of the isopycnals on the shelf side of the flow, which is noticeable in the density structure of Fig. 11 (note how 26.9 in section 03 and 26.85 in section 02 upwell close to the shelf break). The buoyancy-driven circulation over the shelf is associated with the Western Iberia Buoyant Plume (WIBP) (see the low salinity shelf waters in both sections shown in Fig. 11). The WIBP is a low salinity surface water body fed by the winter-intensified runoff from several rivers on the northwest coast of Portugal and Spain (Fig. 1). During non-upwelling winter conditions, the plume is confined to the inner-shelf from the Mondego river mouth northward and is defined by salinity values under 35.7–35.8. Salinity minima are variable and are usually organized in patches close to the estuaries. Because of their relatively higher buoyancy, the waters of the surface plume limit thermally-driven convection to a thin layer. This contributes to thermal stratification within the plume and to significant cooling: the plume waters usually have lower temperatures than those offshore (note the colder band close to the coast in Fig. 5 and to the north of the Douro in Fig. 10). During upwelling-favorable conditions the plume is stretched offshore and, as a result of its lower

temperatures, it often masks the warm signature of the IPC, as in the cases reported by Oliveira et al. (2004) and Santos et al. (2004). Through this mechanism the surface signature of the IPC may disappear, giving the false impression that the current has weakened or reversed.

5.3. Separation of the IPC

Mazé et al. (1997) showed that at both Mediterranean and Central Water levels a significant transport out of the Iberian Basin may occur west of the Galicia Bank. The authors hypothesized that part of this transport may originate from a separation of the poleward current north of the Aveiro Canyon (Daniault et al., 1994), recirculating around the bank and re-entering the basin. A section from May 1998 (Fig. 12, Sec N of Fig. 2 from IPIMAR cruise 02070598) shows a light water core well off the slope with relatively high salinity (more than 36.0) and higher temperatures (around 15 °C) 100–150 m deep. This warm and salty surface water can be observed 200 km offshore in a zone slightly to the south of the Galicia Bank (see Fig. 1). This surface pattern has a corresponding high salinity anomaly at Mediterranean Water levels (see salinity and temperature at 900 m) indicating that part of the Mediterranean Water core may also have been displaced offshore. In fact the entire vertical structure usually observed attached to the slope, including the salinity minimum at 500 m depth, is repeated offshore. On the other hand, in Fig. 12, the slope zone shows no clear evidence of the IPC. A close observation of the temperature and salinity sections indicates that an upwelling event has developed before the survey. On the upper slope the isopycnals and the isotherms upwell. Also, the upper layer (0–50 m) has lower salinity values which originate on the shelf as a consequence of the offshore transport of the WIBP. Vitorino et al. (2002) report a series of measurements on the shelf at about 41°N that confirm the occurrence of several upwelling episodes in mid-April and during the first week of May 1998, just before the section in Fig. 12, with shelf currents above 30 cm/s.

We may speculate that the observed structure (Fig. 12) corresponds to a transient detachment of the IPC based on the fact that over the slope there are no clear signs of the warm tongue. However, we have no additional means to confirm this, and the hypothesis that the observed structure is associated with a separated slope water eddy should not be discounted.

5.4. Eddy shedding

Interaction of poleward-slope currents with topography promotes transient flow separation and eddy shedding. Examples of such a process are reported for the southern Bay of Biscay by Pingree and LeCann (1992a). These authors introduced the term SWODDIES (Slope Water Oceanic EDDIES) to describe anticyclones, sometimes with one or two cyclonic companions, that form during the separation of a poleward slope current at a number of the more prominent capes along northern Iberia and southern France. These are long-lived (up to 1 year) features with depths of over 1000 meters, that migrate offslope into the deep ocean. One case off Western Iberia is described in Pingree and LeCann (1993). Evidence of meanders and eddies related to the presence of the Poleward Current at the Western Iberia margin are reported in Fiúza et al. (1998) and Oliveira et al. (2004).

An example of the evolution of the Iberian Poleward Current warm tongue for the winter of 2002 is provided in Fig. 13. At the beginning of January (Fig. 13a) the warm tongue is intense and it is possible to observe the initial stage of the SWODDY as the result of the evolution of an unstable feature centered at about 10°W, 40°N in the zone between the Nazaré and Aveiro Canyons. A week later (Fig. 13b), two conspicuous warm eddies (and a meander centered at about 41.5°N) are noticeable off the Portuguese coast indicating the presence of two anticyclones of about 40 km diameter. Both structures appear to have smaller cyclonic counter-parts to their southern flank.

An example of eddy separation is provided in Figs. 10 and 14. The thermal images correspond to situations occurring on 28 January and 9 February of 1997. The warmer waters (in darker tones) are

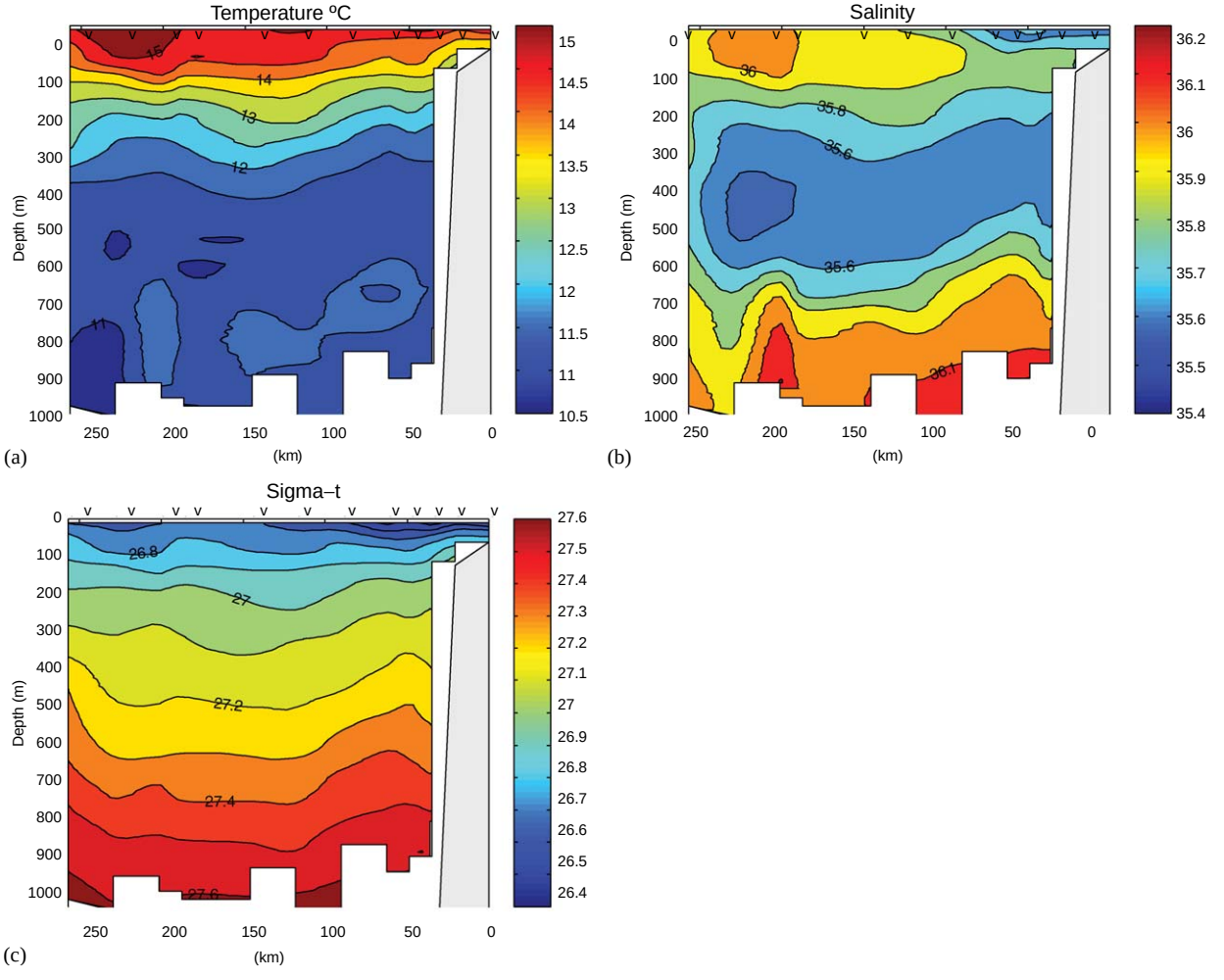

Fig. 12. Vertical distributions of temperature, salinity and density anomaly ($kg\,m^{-3}$) along section N (Fig. 2).

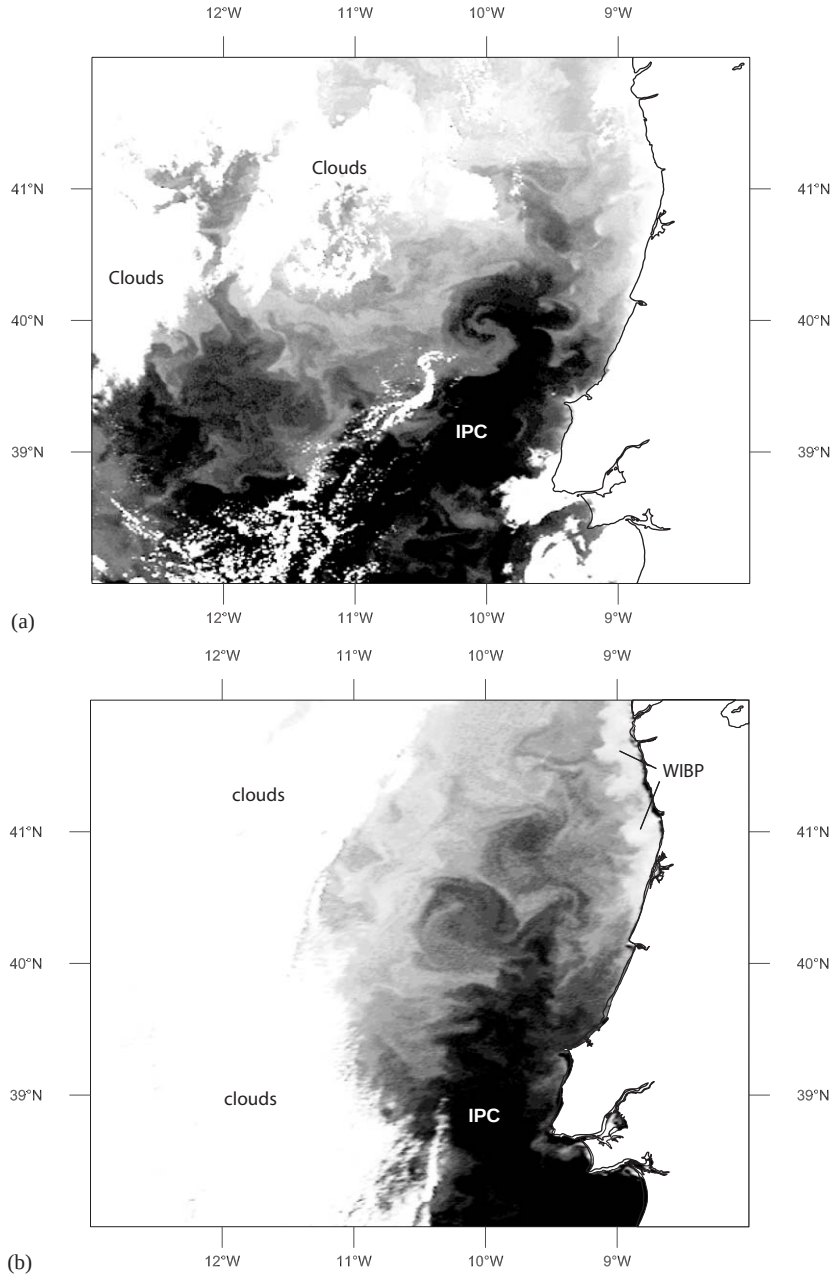

Fig. 13. Two stages of the evolution of the IPC warm tongue off Portuguese west coast during winter of 2002 depicting the generation of instabilities and a slope water anticyclone (swoddy). The images correspond to channel 4 brightness temperatures from AVHRR data for: (a) 09/01/02 (03:08 UTM); (b) 16/01/02 (13:28 UTM); The darker tones represent higher temperatures. Greyshade intensity was chosen to enhance the turbulent features.

penetrating northward and several eddies and smaller scale instabilities can be observed. In the first image (Fig. 10) two dipolar structures are visible. The larger of the two (marked A) consists of a small cyclone and an anticyclone that is zonally stretched. After 12 days (Fig. 14) the

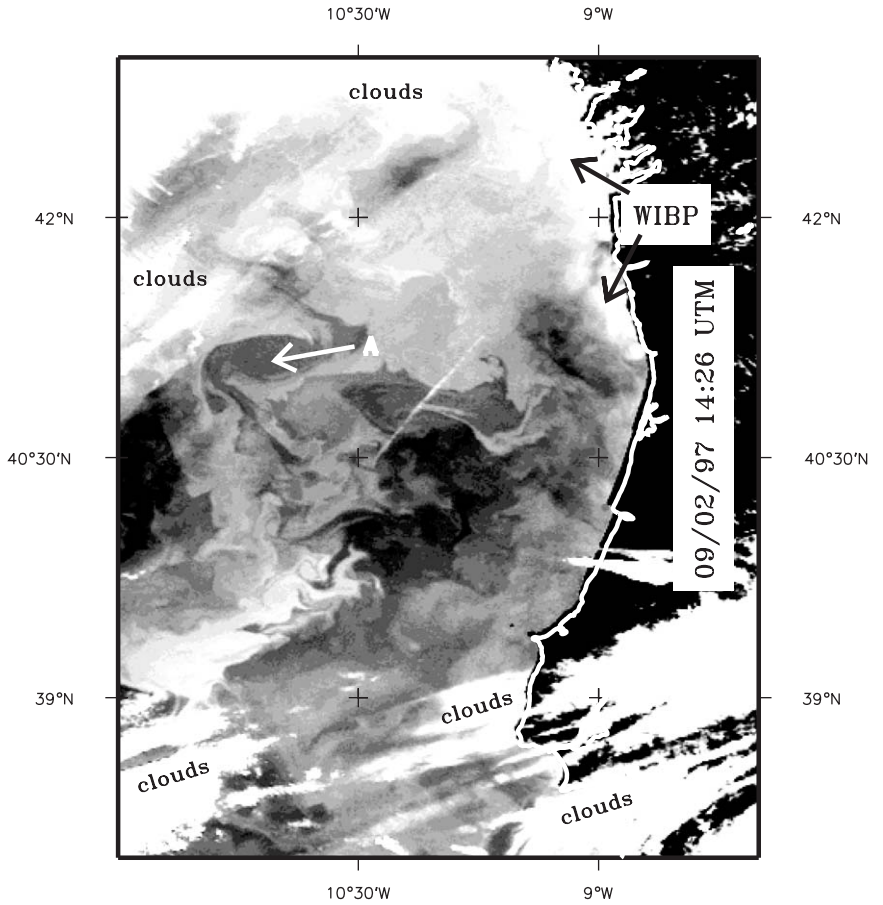

Fig. 14. AVHRR brightness temperature image of 09/02/97 (14:26 UTM) showing the western Iberian offshore. Darker tones correspond to warmer waters. A surface anticyclone, corresponding to a separated eddy approximately in the middle of the domain is marked (A). Areas affected by clouds are marked.

dipole has separated and migrated northwest to 41°N, 11°W with an average displacement of about 9 km/day (0.1 m/s). Other turbulent structures are created during the course of this process.

A detailed study of the generation and evolution of the poleward slope-flow along the western Iberia Margin (Iberian Poleward Current) and its interaction with topography was conducted by Peliz et al. (2003b). Eddy shedding may occur as a result of the separation of the flow downstream of the topography, and as a result of the evolution of unstable regimes created in the process of interaction of the flow with the topography. Peliz et al. (2003b) describe several examples of eddy shedding. The authors show that the vertical sheared flow past topographic discontinuities like the Estremadura Promontory or the Aveiro Canyon generates several anticyclones usually accompanied by one or more cyclones. Dipolar interaction promotes the detachment of a number of structures offshore. This turbulent character of the IPC also acts to drain energy from the mean flow and erodes the slope current, exporting a proportion of the kinetic energy offshore.

Yearly composites of the number of winter (January–March) positive SLA occurrences are shown in Fig. 15 (associated average mapping error is shown in Fig. 16). Interannual variability

in the frequency of anticyclone occurrences is evident. The winters of 1996–1998 show a particularly high number of occurrences, especially in the southwest. On the other side, 1999 and 2000 have relatively low values. It is particularly interesting to notice that in 1999 the occurrences east of 12°W are low. We recall that the analysis of individual AVHRR images indicates that 1996–1998 was a period of significant IPC activity in contrast to 1999 and 2000. In this context, we can speculate that the differences in the eddy activity registered between both periods may be associated on one hand with higher frontal activity and on the other hand with a higher number of eddies shed off Western Iberia as a consequence of the IPC mesoscale activity.

Isolated offshore eddies are expected to migrate westward because of the β effect. The westward migration of significant sea surface height anomalies is apparent not only where sea surface elevation anomalies are frequent ($\sim 35°$N) but also offshore of Western Iberia. Fig. 17 shows a longitude-time plot of such surface height anomalies. In the case of Western Iberia, westward propagation is significant west of 12°W. The black line in the middle of the plot corresponds to a westward phase speed of 0.016 m/s which is slightly above that estimated by theoretical considerations. The maximum zonal phase speed for a mode 1 baroclinic planetary wave is $c_x = -\beta R_i^2$, where $R_i = NH/\pi f_0$ corresponds to the first internal Rossby radius and f_0 is an average Coriolis parameter for the zone (e.g., Gill, 1982). Using the density data from the April cruise (Fig. 3) where the upper 1000 m are almost linearly stratified, $N = 0.0027\,\mathrm{s}^{-1}$, and taking an interval for the vertical structure $H = [2500, 3000]$, we obtain a Rossby radius around 22,26 km (accurate estimates from Chelton et al. (1998) give $R_i = 25$ km). The corresponding estimates for c_x are within the interval $[0.009, 0.014]\,\mathrm{ms}^{-1}$. A thorough analysis of the westward propagation of features in this region is given by Pingree (2003). The important fact to note is that westward propagation of features is observed, and that many of these are generated during the process of detachment from the slope, especially when the poleward flow is stronger.

6. Discussion

According to Frouin et al. (1990) the IPC is a seasonal flow, and its seasonality is above all related to the seasonal changes in wind forcing. Haynes and Barton (1990) report the results from an observational program conducted at the end of the 1986 upwelling season (summer). The authors show a significant correlation between the wind and current fields, and interpret the weakening of the surface poleward current as a response to the wind burst. Nevertheless, off slope, a surface drifter (their buoy 6220 in Fig. 8) indicates that the poleward current was still present off the shelf and slope.

Additional data presented here support previous work but stress the relevance of the density-driven component of the IPC. The core of the IPC is found over the slope and sometimes strong meanders and eddies extend into deeper waters. The current has been measured at large distances from the shelf edge (~ 70 km). From the data presented there is no clear evidence that the poleward flow reverses or becomes an undercurrent in response to changes in the local wind stress. Peliz et al. (2003a) conducted a numerical study aiming to test the response of a slope flow with characteristics similar to the IPC on week-to-month-scale wind events. They concluded that the slope flow has a considerable degree of independence and might coexist with relatively strong equatorward upwelling currents over the shelf and upper slope. In the case of intense winds the slope current may decrease in intensity and its surface core may move offshore a few kilometers (usually to non-sampled areas in coastal surveys). Nevertheless, events at these scales do not strongly modify the structure of the current. Two winter observational programs (Jorge da Silva, 1988; Santos et al., 2004) report the presence of the IPC despite the fact that they were preceded by or occurred during significant upwelling events.

During summer the signs of the IPC are generally weak. However, the transition process to the summer regime is not clear. No indications about the reversal or deepening of the current were obtained. On the other hand we speculate that part of the flow may be advected offshore (Section 5.1).

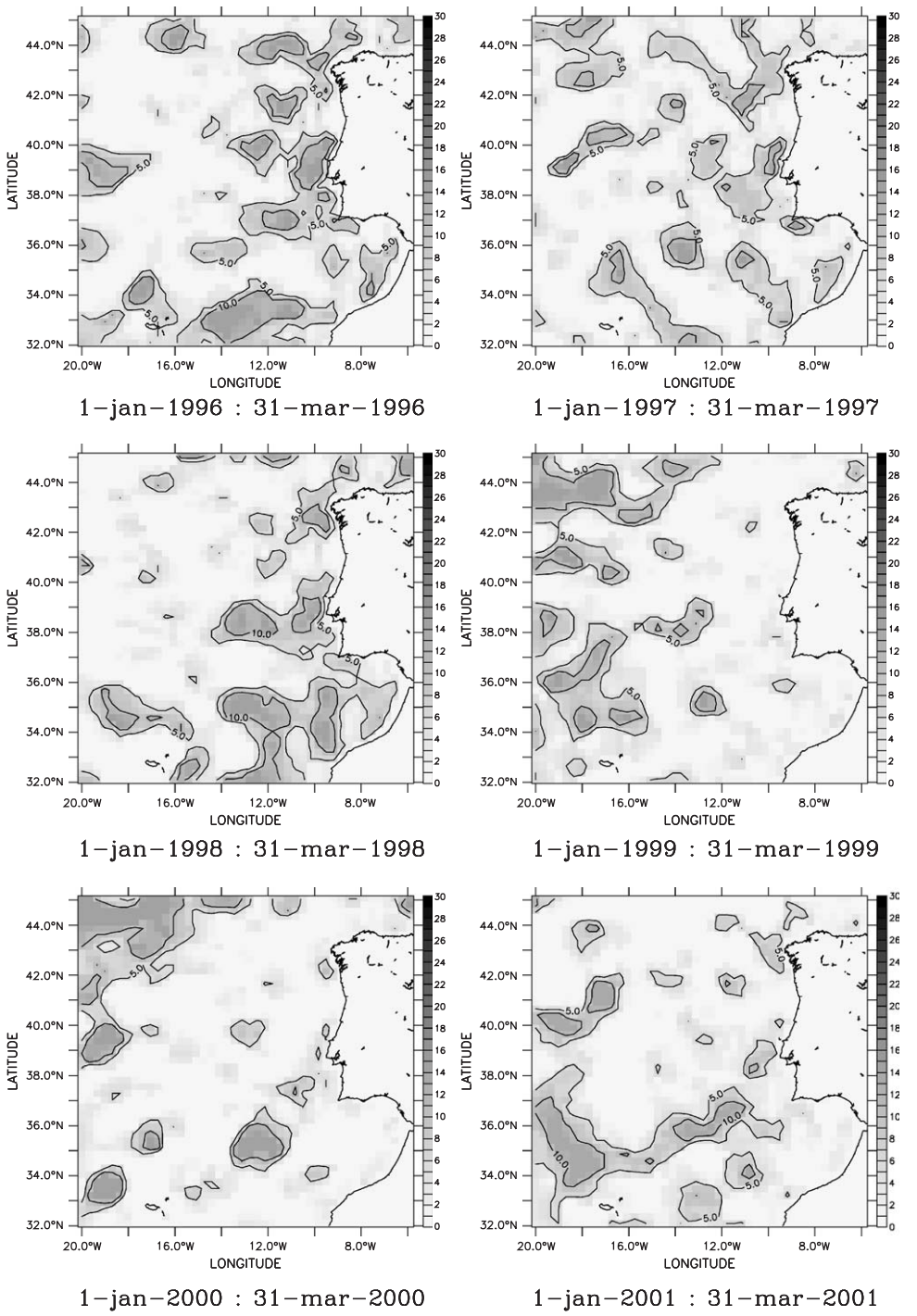

Fig. 15. Yearly distribution of occurrences of positive (anticyclonic) sea level anomalies for the winter months (January–March) for the period 1996–2001.

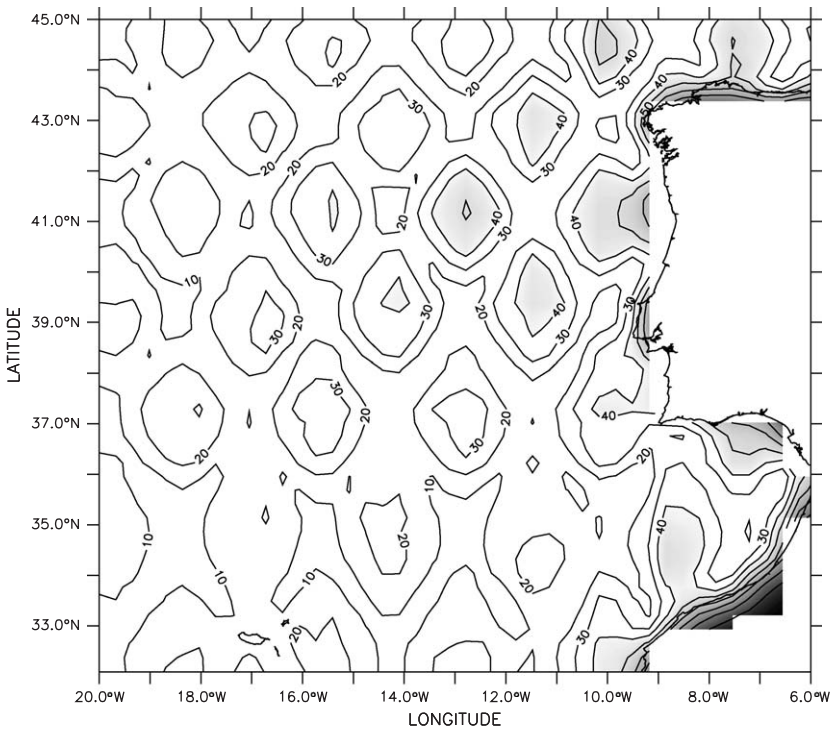

Fig. 16. Map of average formal mapping error for the period from 1 January 1995 to 31 December 2000. Areas of with mapping error greater than 40% are shaded. The figure shows that higher mapping errors are concentrated in the coastal areas and in the middle of the diamonds delimited by satellite ground tracks. Lower errors are found between 34N and 36N.

Peliz et al. (2002) present the results of a summer hydrological survey after a long upwelling event, where there is evidence of a warm and salty current which the authors attribute to a remnant of the IPC. Very close to the shelf edge Poleward Flows were registered all year round even during persistent upwelling.

With the arguments above we formulate a new hypothesis for the evolution and seasonality of the IPC that accounts not only for the wind forcing itself, but also for the variability of the upper ocean density gradients which in our view constitute the main mechanism forcing the slope flow. The seasonal cycle of development and decay of an IPC involves two phases:

I - Development phase

- Strengthening of the meridional density gradients during late fall and winter (Section 4.3).
- Development of the IPC as a tongue-like structure as described in Frouin et al. (1990), Dubert (1998) and Peliz et al. (2003a).
- Development of the turbulent character of the IPC (e.g., Peliz et al., 2003b; Section 5.4).

II - Decay phase

- Weakening of the meridional density gradients in late winter (Section 4.1).
- Broadening of the warm tongue and erosion of the near-surface thermohaline structure by the action of wind stress and interactions in the mesoscale eddy field (Section 5.4).
- Offshore drift of the tongue and individual eddies by dipolar interaction (Peliz et al., 2003b) and the action of the β effect. Eventually the separation of the slope flow can be observed north of the Aveiro Canyon (Section 5.3).
- Increase of upwelling dynamics on the upper slope and shelf during summer (Section 5.1).

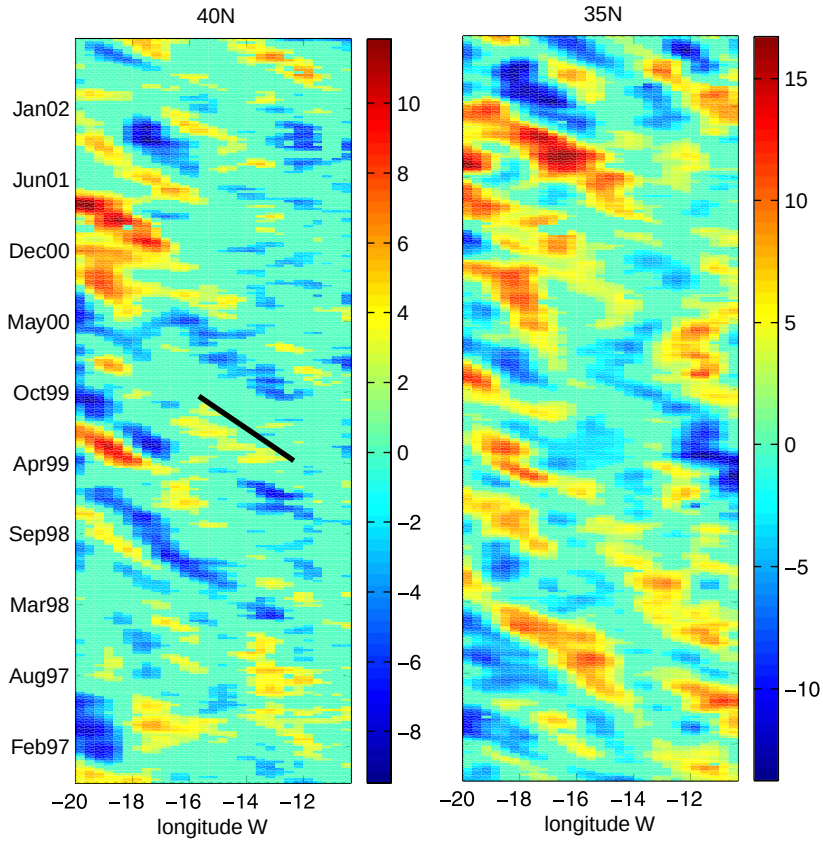

Fig. 17. Time-longitude plots of significant SLA (cm) for a zonal line at 40°N (left) and 35°N (right). A thick line on the left side indicates a phase velocity of 0.016 m/s.

During the peak of upwelling activity (July–September) the warm tongue is not observed at the surface once the near-surface layer is strongly heated. Besides, shelf break filaments develop. Nevertheless, poleward currents along the slope are observed (see Section 5.1) but are possibly integrated into the upwelling current system (an upwelling countercurrent). Some of the remaining eddy structures can last until the summer and interact with the filaments (Peliz et al., 2002).

7. Conclusion

To conclude we present a hypothetical scheme of the upper ocean winter circulation in the Iberia Basin, based on the above discussion. Fig. 18 does not concern any particular observational period. Instead, it is an attempt to illustrate and systematize the winter circulation features referred to in the literature, and those recurrently observed in hydrology observations and satellite data.

The Iberian Basin is separated into two distinct areas. A northern area where the large-scale flow is predominantly southward with the presence of the Portugal Current (PoC 1). In this northern area the poleward flow is confined to the vicinity of the slope. To the west, between the Galicia Bank and the coast, southward cold intrusions are recurrently observed and are represented here as an eastern branch of the Portugal Current (2).

The frontal system recurrent in the SST imagery (Section 4) is represented at about 39–40°N (3). The term Western Iberia Winter Fronts (WIWiFs)

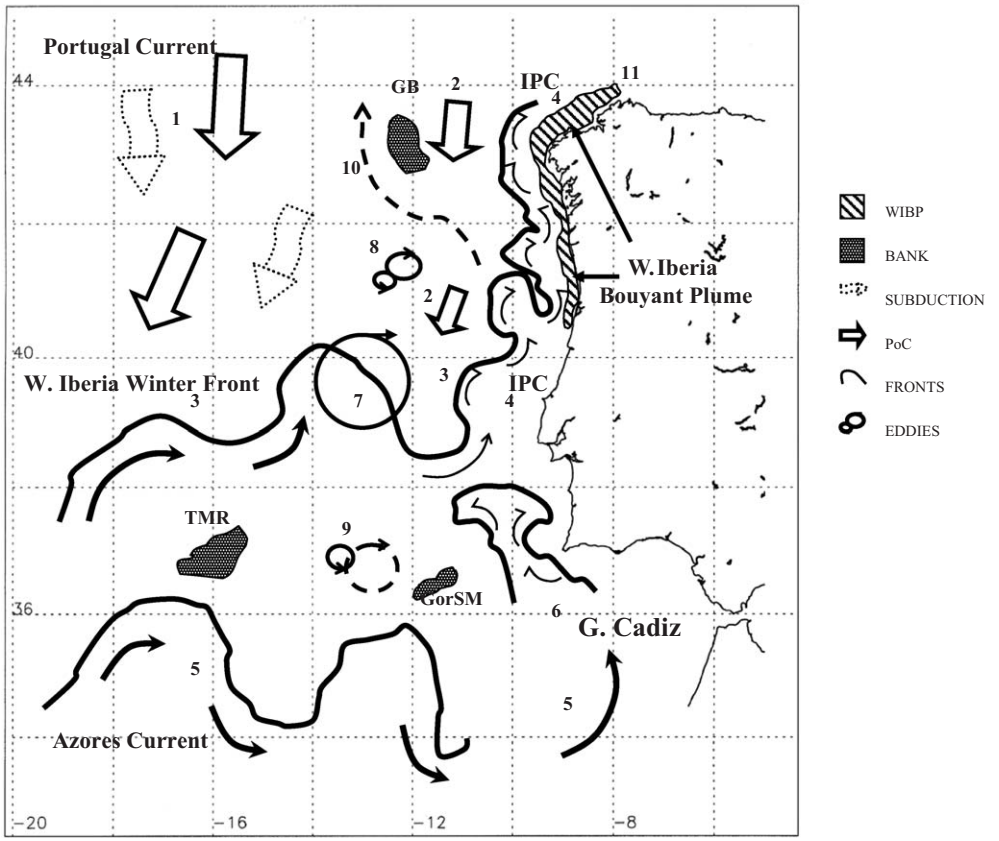

Fig. 18. Scheme of upper ocean winter-time circulation in the Western Iberian Basin. 1—Portugal Current (PoC), 2—Portugal Current Eastern Branch, 3—Western Iberia Winter Front (WIWiF), 4—Iberian Poleward Current (IPC), 5—Azores Current Eastern Branch (ACEB), 6—Gulf of Cadiz northern recirculation, 7—Recurrent anticyclonic meander/eddy, 8—Swoddies, 9—Meddies and companion cyclones, 10—IPC alternative path/branch, 11—Western Iberia Buoyant Plume (WIBP).

is proposed to describe the recurrent fronts at these latitudes. They represent the transition to the southern area of the Iberian Basin where the PoC is less influential and an eastward advection of relatively warm and salty waters becomes important and constitutes the main generation mechanism of the poleward flow. In the vicinity of the coast this front is deflected northward, generating the Iberian Poleward Current (IPC, 4).

A second frontal system (5) south of 36°N represents the eastern end of the Azores Current (AC). Feature (6) is a warm inflow into the basin from the Gulf of Cadiz. This recurrent warm signature in SST satellite imagery is likely to be a northward recirculation of the AC, and is possibly connected with the IPC (Section 4.2).

Fig. 18 also shows schematic representations of the types of mesoscale features found in the area: (7) the large meanders on the WIWiF (including a recurrent large anticyclonic meander (see for example Fig. 5)), (8) SWODDIES, and (9) the surface expression of MEDDIES. Finally, the branch (or transient path) of the IPC as discussed in Section 5 (10) is also represented.

The Western Iberia Buoyant Plume (WIBP - 11) is shown as a narrow coastal band which in some cases may be associated with strong poleward transport over the shelf.

This winter circulation scheme, though supported by previous studies and the many observations shown in the preceding sections, still has

many aspects that need further research. There are certain open questions that require detailed observational and modelling work, namely: (i) The circulation at the eastern end of the Azores Current and the origin of the frontal system off Western Iberia. The existing models are in some cases contradictory for this area. The fate of the AC at the eastern margin and its possible connection to the WIWiFs has been discussed in this paper, however the evidence is not conclusive and should be investigated. (ii) The northward recirculation of the AC in the Gulf of Cadiz together with the mechanism proposed by Mauritzen et al. (2001) may induce an important salinity flux, and explain the higher salinites in the upper waters of the Western Iberian Basin. (iii) The hypothesis regarding the seasonality of the IPC needs to be tested. The transition between winter and summer regimes off western Iberia has never been properly investigated. (iv) Clear evidence of the separation or branching of the IPC following the findings of Mazé et al. (1997) is still lacking. Finally (v), evidence of interannual variability has been reported in this study. The source of controversy in some of the models may be inherent to long-term fluctuations. In some years the AC and WIWiF appear to be weaker (northern regime). Then, it is expected that the PoC dominates the offshore circulation of the Iberian Basin and a lower IPC transport is noticeable. This regime is in agreement with the circulation schemes proposed by Paillet and Mercier (1997). In other years, the frontal systems may intensify (southern regime) and poleward advection of southern waters becomes more significant following the circulation scheme described by Ríos et al. (1992). Pingree (2003) report this interannual variability and relate it to the varying intensity of the North Atlantic Gyre. A weakened gyre such as for years 1996–1998 is observed in periods of low NAO index and is associated with lower recirculation of the NAC southward, enabling a warming of the European Continental Slope zones. In years of strong North Atlantic Gyre, the opposite is observed. Our results indicate that the relationship between NAO and zonal SST gradients is not linear being possibly associated with regime fluctuations. More detailed work is needed to support the hypothesis of meridional variations in these frontal systems.

Acknowledgements

This paper was supported by the following projects: SURVIVAL (FCT/PRAXIS/P/CTE/11282/98), PELAGICOS (FCT PLE/13/00), SARDYN (EU Q5RS 2002-000818) and SIGAP (22-05-01-FDR-00013). CTD data used in the paper originate from several observational IPIMAR programmes. NCEP Reanalysis data were provided by the NOAA-CIRES Climate Diagnostics Center, Boulder, Colorado, USA, from their Web site at http://www.cdc.noaa.gov/. Altimetry products were produced by the CLS Space Oceanography division as part of the Environment and Climate EU ENACT project (ENVH2 - CT 2001-0117) and with support from CNES. SST data were obtained from the NASA Physical Oceanography Distributed Active Archive Center at the Jet Propulsion Laboratory, California Institute of Technology. Our thanks to Evan Mason for his editorial support. The comments of the reviewers have significantly contributed to the quality of this paper.

References

Alonso, J., de Castillejo, F.F., Diaz del Rio, G., Marcote, D., Casas, G., 1995. Preliminary Results of Current Measurements in the North West of the Iberian Peninsula, MORENA Scientific and Technical Report no 15, Instituto Espanol de Oceanografia C.O., La Coruna, Spain.

Arhan, M., Colin de Verdière, A., Mémery, A., 1994. The eastern boundary of the subtropical North Atlantic. Journal of Physical Oceanography 24, 1295–1316.

Armi, L., Stommel, H., 1983. Four views of a portion of the North Atlantic Subtropical Gyre. Journal of Physical Oceanography 13, 828–857.

Brügge, B., 1995. Near-surface mean circulation and kinetic energy in the central North Atlantic from drifter data. Journal of Geophysical Research 100, 20543–20554.

Cayula, J.-F., Cornillon, P., 1992. Edge detection algorithm for SST images. Journal of Atmospheric and Oceanic Technology 9, 67–80.

Chelton, D.B., deSzoeke, R.A., Schlax, M.G., El Naggar, K., Siwertz, N., 1998. Geographical variability of the first-baroclinic Rossby radius of deformation. Journal of Physical Oceanography 28, 433–460.

Daniault, N., Mazé, J.P., Arhan, M., 1994. Circulation and mixing of Mediterranean Water west of Iberian Peninsula. Deep Sea Research I 41, 1685–1714.

Dubert, J., 1998. Dynamique du Système de Courants vers le Pôle au Voisinage de la Pente Continentale à l'Ouest et au Nord de la Péninsule Ibérique. Ph.D. Thesis, University of Bretagne Occidentale, 237 pp.

Ducet, N., Le Traon, P.-Y., Reverdin, G., 2000. Global high resolution mapping of ocean circulation from TOPEX/Poseidon and ERS-1/2. Journal of Geophysical Research 105, 19477–19498.

Fiúza, A.F.G., Hammann, M., Ambar, I., Días del Río, G., González, M., Cabanas, J.M., 1998. Water masses and their circulation off western Iberia during May 1993. Deep Sea Research I 45, 1127–1160.

Frouin, R., Fiúza, A.F., Ambar, I., Boyd, T.J., 1990. Observations of a Poleward Surface Current off the Coast of Portugal and Spain during winter. Journal of Geophysical Research 95, 679–691.

Garcia-Soto, C., Pingree, R.D., Valdés, L., 2002. Navidad development in the southern Bay of Biscay: climate change and swoddy structure from remote sensing and in situ measurements. Journal of Geophysical Research 107 (C8) doi:10.1029/2001JC001012.

Gill, A.E., 1982. Atmosphere-Ocean Dynamics. Academic Press, New York, 662 pp.

Halpern, D., 1991. The NASA Ocean Data System at the Jet Propulsion Laboratory. Advanced Space Research 11, 3255–3262.

Haynes, R., Barton, E.D., 1990. A Poleward Flow along the Atlantic Coast of the Iberian Peninsula. Journal of Geophysical Research 95, 11425–11441.

Haynes, R., Barton, E.D., Pilling, I., 1993. Development, persistence and variability of upwelling filaments off the Atlantic Coast of the Iberian Peninsula. Journal of Geophysical Research 98, 22681–22692.

Jia, Y., 2000. Formation of an Azores Current due to the Mediterranean overflow in a modelling study of the North Atlantic. Journal of Physical Oceanography 30, 2342–2358.

Jones, P.D., Jonsson, T., Wheeler, D., 1997. Extension to the North Atlantic Oscillation using early instrumental pressure observations from Gibraltar and South-West Iceland. International Journal of Climatology 17, 1433–1450.

Jorge da Silva, A., 1988. Contribuição do Inst. Hidrográfico para o projecto JNICT 87344. Resultados do Cruzeiro CECIR XV Dezembro 1988 (Hydrographic Institute CECIR XV cruise report). IH, Lisboa 35 pp. [REL TF-OF-2/93]

Krauss, W., 1986. The North Atlantic Current. Journal of Geophysical Research 94, 6159–6168.

Mauritzen, C., Morel, Y., Paillet, J., 2001. On the influence of Mediterranean Water on the Central Waters of the North Atlantic Ocean. Deep Sea Research I 48, 347–381.

Mazé, J.P., Arhan, M., Mercier, H., 1997. Volume budget of the eastern boundary layer off the Iberian Peninsula. Deep Sea Research I 44, 1543–1574.

New, A.L., Jia, Y., Coulibaly, M., Dengg, J., 2001. On the role of the Azores Current in the ventilation of the North Atlantic Ocean. Progress in Oceanography 48, 163–194.

Oliveira, P.B., Serra, N., Fiúza, A.F.G., Ambar, I., 2000. A study of meddies using simultaneous in-situ and satellite observations. In: David, Halpern (Ed.), Satellite Oceanography and Society. Elsevier Science, Amsterdam, pp. 125–148.

Oliveira, P.B., Peliz, A., Dubert, J., Rosa, T., Santos, A.M.P., 2004. Winter geostrophic currents and eddies in the western Iberia coastal transition zone. Deep Sea Research I 51, 367–381.

Özgökmen, T.M., Chassignet, E.P., Rooth, C.G., 2001. On the connection between the Mediterranean Outflow and the Azores Current. Journal of Physical Oceanography 31, 461–480.

Paillet, J., Arhan, M., 1996. Shallow pycnoclines and mode water subduction in the eastern North Atlantic. Journal of Physical Oceanography 26, 96–114.

Paillet, J., Mercier, H., 1997. An inverse model of the eastern North Atlantic general circulation and thermocline ventilation. Deep-Sea Research I 44, 1293–1328.

Peliz, A., Rosa, T., Santos, A.M.P., Pissarra, J., 2002. Fronts, jets, and counter-flows in the Western Iberia Upwelling System. Journal of Marine Systems 35, 61–77.

Peliz, A., Dubert, J., Haidvogel, D.B., 2003a. Subinertial response of a density-driven Eastern Boundary Poleward Current to wind forcing. Journal of Physical Oceanography 33, 1633–1650.

Peliz, A., Dubert, J., Haidvogel, D.B., Le Cann, 2003b.Generation and unstable evolution of a Density-Driven Eastern Poleward Current. Journal of Geophysical Research 108 (C8), 3268. doi:10.1029/2002JC001443.

Penduff, T., Colin. de Verdière, A., Barnier, B., 2001. General circulation and intergyre dynamics in the eastern North Atlantic from a regional primitive equation model. Journal of Geophysical Research 106, 22313–22329.

Pérez, F.F., Castro, C.G., Álvarez-Salgado, X.A., Ríos, A., 2001. Coupling between the Iberian Basin-scale circulation and the Portugal boundary current system: a chemical study. Deep Sea Research I 48, 1519–1533.

Pingree, R., 1997. The Eastern Subtropical Gyre: flow, rings, recirculations, structure and subduction. Journal of Marine Biology Association U.K. 77, 573–624.

Pingree, R., 2003. Ocean structure and climate (Eastern North Atlantic): in situ measurements and remote sensing (altimeter). Journal of the Marine Biological Association of the United Kingdom 82, 681–707.

Pingree, R., Le Cann, B., 1992a. Three anticyclonic Slope Water Oceanic eDDIES (SWODDIES) in the Southern Bay of Biscay in 1990. Deep Sea Research I 39, 1147–1175.

Pingree, R., Le Cann, B., 1992b. Anticyclonic eddy X91 in the southern Bay of Biscay, May 1991 to February 1992. Journal of Geophysical Research 97, 14353–14367.

Pingree, R., Le Cann, B., 1993. A shallow Meddy (a Smeddy) from the secondary Mediterranean Salinity Maximum. Journal of Geophysical Research 98, 20169–20185.

Pollard, R.T., Pu, S., 1985. Structure and Circulation of the upper Atlantic Ocean northeast of Azores. Progress in Oceanography 14, 443–462.

Richardson, P.L., Bower, A., Zenk, W., 2000. A census of meddies tracked by floats. Progress in Oceanography 45, 209–250.

Ríos, A., Pérez, F., Fraga, F., 1992. Water Masses in the upper and middle North Atlantic Ocean East of the Azores. Deep Sea Research 39 (3/4), 645–658.

Rosenfeld, L.K., 1983. WHOI technical report, 85-35, 21.

Santos, A.M.P., Peliz, A., Dubert, J., Oliveira, P.B., Angelico, M.M., Re, P., 2004. Impact of a winter upwelling event on the distribution and transport of sardine eggs and larvae off western Iberia: a retention mechanism. Continental Shelf Research 24(2), 149–165.

Saunders, P.M., 1982. Circulation in the Eastern North Atlantic. Journal of Marine Research 40, 641–657.

Serra, N., Ambar, I., 2002. Eddy generation in the Mediterranean undercurrent. Deep Sea Research II 49, 4225–4243.

Smith, E., Vazquez, J., Tran, A., Sumagaysay, R., 1996. Satellite-derived sea surface temperature data available from the NOAA/NASA Pathfinder Program. EOS. American Geophysical Union. URL: http://www.agu.org/-eos_elec/95274e.html.

Stammer, D., Hinrichsen, H.-H., Käse, R., 1991. Can meddies be detected by satellite altimetry? Journal of Geophysical Research 96, 7005–7014.

Sy, A., 1988. Investigation of large-scale circulation patterns in the Central North Atlantic: the North Atlantic Current, the Azores Current, and the Mediterranean Water Plume in the area of the Mid-Atlantic Ridge. Deep Sea Research 35, 383–413.

Van Aken, H.M., 2001. The hydrography of the mid-latitude Northeast Atlantic Ocean—Part III: the subducted thermocline water mass. Deep Sea Research I 48, 237–267.

Vitorino, J., 1995. Resultados do cruseiro CECIR XVII. [CECIR XVII cruize report]. Instituto Hidrográfico, unpublished manuscript.

Vitorino, J., Oliveira, A., Jouanneau, J.M., Drago, T., 2002. Winter dynamics on the northern Portuguese shelf. Part 1: physical processes. Progress in Oceanography 52, 129–153.